Proceedings of the XI DINAME, 28th February-4th March, 2005 - Ouro Preto - MG - Brazil
Edited by D.A. Rade and V. Steffen Jr.

MODES AND REGULAR SHAPES. HOW TO EXTEND COMPONENT MODE SYNTHESIS THEORY.

Etienne Balmes

SDTools and Ecole Centrale Paris MSSMat, 92295 Chatenay Malabry France
balmes@sdtools.com

Abstract This paper gives an integrated perspective on modes and other regular shapes that have been classically used in modal analysis, modeshape expansion, component mode synthesis, domain decomposition, ... Illustrations are taken out of three application areas: parameterized models which are typically considered in finite element updating and uncertainty propagation applications, hybrid models coupling test and analysis information, and design of structures damped using viscoelastic materials.

Keywords*: reduction, substructuring, superelement, optimization, damping*

1 Introduction

The notion of modes is central to the analysis of low frequency dynamics. They are routinely measured and they have unique numerical properties that makes them a fundamental tool in numerical simulations. A first section gives a unified perspective of classical Component Mode Synthesis results (Craig, 1987). The introduction of normal modes and classical static shapes (constraint modes, attachment modes, residual attachment modes) is motivated by the need to approximate the dynamics flexibility for a restricted set of inputs and a know frequency range. The following sections illustrate the usefulness of diverging from this classical theory. To help in the formulation of new reduction methods, two basic methodologies for a priori error estimation (Balmes, 1996a) and subspace classification (Balmes, 1996b) are introduced.

Considering multiple models is a first classical deviation from CMS theory (Balmes, 1996c). Parameterized finite element models are commonly used in FE model updating (Bobillot, 2002), uncertainty propagation (Balmes, 2004b), or design of structures (Balmes and Germès, 2002). The case of uncertainty predictions on the modal properties of an Ariane 5 upper stage model are used in section 3 to illustrates applicable model reduction techniques.

Using an imperfect model in combination with good quality measurements is a second deviation. This is particularly useful in experimental modal analysis applications where one needs to estimate unmeasured quantities while not having a high quality model available. The application of enhanced Structural Dynamics Modification (SDM) methods to a motor pump (Corus, 2003) is used to illustrate current research issues in the use of hybrid test/analysis models.

Model reduction with real shapes for structures damped with viscoelastic material is a last deviation that will be illustrated. Although the numerical solvers are simple applications from those introduced to study parametric families of models, there is a tremendous interest in incorporating damping predictions in the structural design process. After a brief overview of models and solvers used to predict damped behavior, one will show how various model reduction techniques are used in practice to allow the numerical optimization of damping devices considered in automotive and aerospace applications (Balmes and Germès, 2002; Verdun and Balmes, 2003).

2 Modes and regular shapes

This section gives a general presentation model reduction techniques that will then be illustrated. Section 2.1 relates model reduction to Ritz-Galerkin methods. Section 2.2 motivates classical free and fixed interface mode bases by the need to build models that are valid for a class of inputs and a given frequency range. Section 2.3 introduces error estimators for reduced model predictions and describes the *Residue Iteration* method that can be used to generate approximate methods with controlled quality in many applications. Finally, section 2.4 shows that modal truncation can be seen as a generalized Singular Value Decomposition and thus be used to classify the importance of directions in a given subspace.

2.1 Ritz analysis for discrete models

In a fairly general setting, models of structural dynamics obtained by the finite element method can be written in the form

$$\begin{aligned}\left[Ms^2+Cs+K\right]_{N\times N}\{q(s)\} &= [b]_{N\times NA}\{u(s)\}_{NA\times 1}\\ \{y(s)\}_{NS\times 1} &= [c]_{NS\times N}\{q(s)\}_{N\times 1}\end{aligned}. \tag{1}$$

In this description two not very classical, and yet very important, parts are

- the decomposition of the discretized loads $F(s)$ as the product of as the product of a fixed input shape matrix $[b]$ specifying the spatial localization of loads and inputs $\{u\}$ describing the frequency/time dependence and
- the definition of physical outputs $\{y\}$ as a linear combination of DOFs $\{q\}$.

Ritz/Galerkin displacement methods seek approximations of the response within a subspace characterized by a matrix T associated with generalized DOFs q_R

$$\{q\}_N = [T]_{N\times NR}\{q_R\}_{NR} \tag{2}$$

Replacing (2) in equation (1) leads to an overdetermined set of equations. The Ritz approximation assumes that the virtual work for displacements in the dual subspace generated by T^T is also zero, thus leading to a *reduced* model

$$\begin{aligned}\left[T^T M T s^2 + T^T C T s + T^T K T\right]_{NR\times NR}\{q_R(s)\} &= \left[T^T b\right]_{NR\times NA}\{u(s)\}_{NA\times 1}\\ \{y(s)\}_{NS\times 1} &= [cT]_{NS\times NR}\{q_R(s)\}_{NR\times 1}\end{aligned} \tag{3}$$

2.2 Classical CMS bases as approximations of the frequency response

Component mode synthesis and model reduction methods provide methods to build appropriate T bases. While there are many ways to justify classical bases (Craig, 1987), useful insight can be gained by saying their validity is associated with two assumptions : the model need only be valid over a restricted frequency band and the number of inputs is limited. In this section, ones sees how these hypotheses can be translated into the need to include modeshapes and static responses into the T basis.

Considering the response of an elastic structure to applied loads $F(s)_N = [b]_{N\times NA}\{u(s)\}_{NA}$, the exact response at a given frequency is given by

$$H(s) = [c]\left[Ms^2 + K\right]^{-1}[b] = [c][Z(s)]^{-1}[b] \tag{4}$$

The dynamic stiffness $Z(s)$ being an analytic rational fraction, it has a set distinct singularities solutions of

$$[Z(\lambda_j)]\{\phi_j\} = \{0\} \tag{5}$$

these are simply known as the *free modes* of the structure. A reduced model should include these shapes to allow for accurate representations of resonances which are associated with the singularities of the dynamic stiffness. The assumption that the model need only be valid over a given frequency range is used for modal truncation : that is the fact that one keeps the modes associated with frequencies within the target frequency band shown as the F_{max} line in figure 1. A point of particular interest is the static response (at $s = 0$). The associated deformation is

$$\{q_0\} = [Z(0)]^{-1}[b]\{u(0)\} = [T_s]\{u(0)\} \tag{6}$$

the vectors of $T(s)$ are called *attachement modes* in the CMS literature (Craig, 1987). A classical problem is the case of free floating structures (structures with rigid body modes). $Z(0)$ is then singular and one defines attachment modes as responses of all modes except the rigid body ones. Methods to compute this response are analysed in (Farhat and Géradin, 1998).

Bases combining free modes and attachment modes are valid over a certain frequency range (truncation of the series of free modes) and certain inputs characterized by b. Thus they use the two initial assumptions. As shown in figure 1, the incorporation of the attachment modes in the basis allows a representation of the low frequency residual flexibility of higher frequency modes that have been truncated.

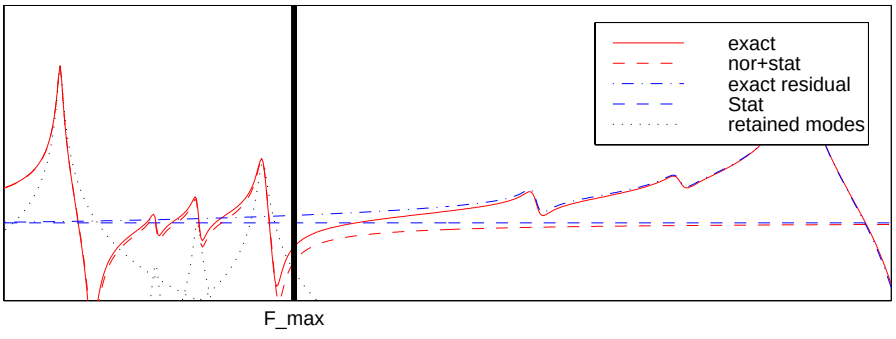

Figure 1: Modes within the band and external contributions

In some applications, the response to applied loads is not particularly representative. One thus considers the response of a structure with enforced displacements on a subset of DOFs. Dividing the DOFs in two groups, active or interface DOFs I and complementary C, leads to

$$\left[\begin{array}{cc} Z_{II}(s) & Z_{IC}(s) \\ Z_{CI}(s) & Z_{CC}(s) \end{array}\right]\left\{\begin{array}{c} < q_I(s) > \\ q_C(s) \end{array}\right\} = \left\{\begin{array}{c} R_I(s) \\ < 0 > \end{array}\right\} \tag{7}$$

where $< >$ denotes a know quantity. The exact solution to this problem is given by

$$\{q\} = [T(s)]\{q_I\} = \left[\begin{array}{c} I \\ -Z_{CC}(s)^{-1}Z_{CI}(s) \end{array}\right]\{q_I\} \tag{8}$$

The subspace found here is frequency dependent and thus can only be used in very restricted applications such as dynamic modeshape expansion (Balmes, 2000). An classical approximation is however found by computing the static (at $s = 0$) value of this subspace

$$[T] = \left[\begin{array}{c} I \\ -K_{CC}^{-1}K_{CI} \end{array}\right] \tag{9}$$

Reduction on this basis is known as static or Guyan condensation (Guyan, 1965). The columns of T are called constraint modes (Craig, 1987). They correspond to unit displacements of the interface DOFs.

Trying to analyze when subspace (9) becomes a poor approximation of subspace (8), it clearly appears that significant deviations can be expected when $Z_{CC}(s)^{-1}$ differs from $Z_{CC}(0)^{-1} = K_{CC}^{-1}$. Such difference is clearly significant for singularities of $Z_{CC}(s)^{-1}$ which are computed by the eigenvalue problem

$$\left[\begin{array}{cc} 0 & 0 \\ 0 & Z_{CC}(\omega_j) \end{array}\right]\left\{\begin{array}{c} 0 \\ \phi_{j,c} \end{array}\right\} = \{0\} \tag{10}$$

This problem defines *fixed interface modes*. The use of a basis combining constraint and fixed attachment modes was proposed in (Craig and Bampton, 1968)

$$[T] = \left[\left[\begin{array}{c} I \\ K_{CC}^{-1}K_{CI} \end{array}\right]\left[\begin{array}{c} 0 \\ \phi_{1:NM,C} \end{array}\right]\right] \tag{11}$$

Here, this appears as the optimal extension of static condensation by incorporation of the singularities of $Z_{CC}(s)^{-1}$ in the reduction basis. The hypothesis on inputs was used when defining inputs. The hypothesis on bandwidth is used to truncate the series of fixed interface modes.

2.3 Error estimates and iterations

Error estimation has been the focus of little attention in substructuring literature while there are classical methods in non linear mechanics. The principle of error estimates on a the solution of a discrete model are rather simple. Knowing an approximate solution $[T]\{q_R\}$, one computes an error residual associated with the fact that the full order solution is not exactly verified by the approximate solution.

For frequency responses (1), the residual is given by

$$R_L = \left[Ms^2 + Cs + K\right][T]\{q_R\} - [b]_{N\times NA}\{u(s)\} \tag{12}$$

Similarly for normal modes the residual is given by

$$R_L = \left[K - \omega_j^2 M\right][T]\{\phi_{jR}\} \tag{13}$$

This residual has the units of a load and thus tends to be very much dependent on the mesh properties and element type. Using an energy norm to measure its size is thus of practical interest in many applications. A reasonable approach is to compute the static response to this load

$$R_D = \left[\hat{K}\right]^{-1} R_L \tag{14}$$

Note that $\left[\hat{K}\right]$ need not be the exact stiffness of the model. It can be a fixed nominal stiffness, a dynamic stiffness or simply a preconditioner (Bobillot, 2002).

The displacement residual leads to a relative error in strain energy

$$\epsilon(\{\phi_j(p)\}, \omega_j(p), p) = \frac{\|R_D\|_{K(p_0)}}{\|\phi_j(p)\|_{K(p_0)}} \tag{15}$$

Error computations shown in section 3.3 are based on this technique. There are strong links between this residual and the Error In Constitutive relations (Chouaki et al., 1998; Barthe et al., 2004).

While measuring the error is interesting, this also provides a very general mechanism to generate approximations with a controlled level of error. The Residue Iteration (RI) method, outlined in figure 2, uses the displacement residual to enrich the subspace $T^{(k+1)} = \left[T^{(k)} \;\; R_D^{(k)}\right]$. In practice, an orthonormalization must be performed before appending $R_D^{(k)}$ to $T^{(k)}$. The need for this orthonormalization is related to the similar step used in conjugate gradient or Lanczos techniques.

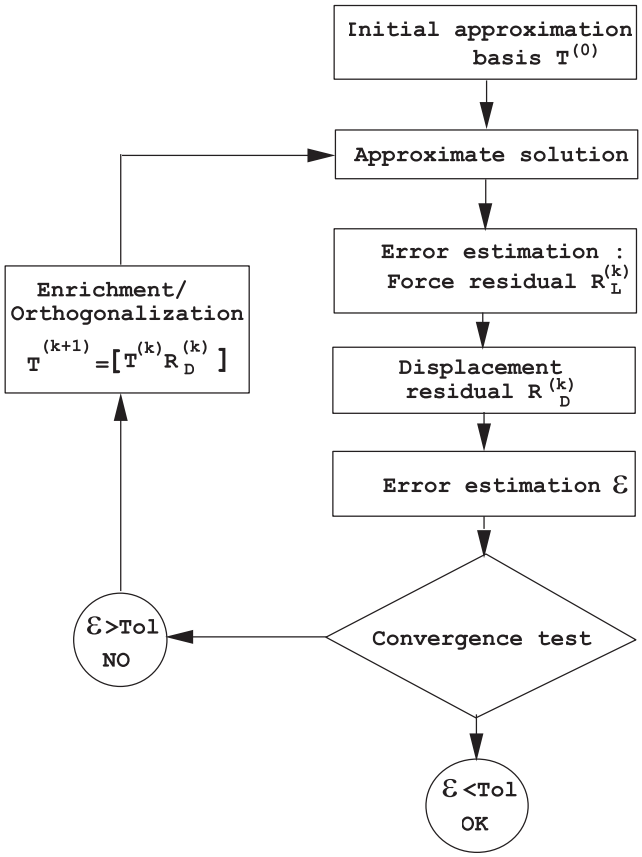

Figure 2: Principle of enrichment strategy of the Residue Iteration Method (Bobillot, 2002).

Variants of the Residue Iteration method have been shown to be efficient for the computation of normal and complex modes (Bobillot, 2002), multiple field problems found in fluid structure interaction and finite element model updating (Bobillot and Balmes, 2002b; Bobillot and Balmes, 2002a), as well as direct frequency response and sensitivities (Kergourlay et al., 2000; Balmes and Germès, 2002; Bobillot and Balmes, 2003).

2.4 Subspace classification and SVD

The Singular Value Decomposition (SVD) is a classical mathematical tool used to select important directions in a given subspace. When confronted with the need to select important directions in a subspace T, it is thus quite interesting to adapt the concepts of SVD.

The general form of an SVD of matrix T is

$$[T]_{N\times NR} = [U]_{N\times N}[S]_{N\times NR}[V]^T_{NR\times NR} \tag{16}$$

where S is a diagonal matrix (the elements of this diagonal are called singular values), and the matrices of right V and left U singular vectors are unitary (the singular vectors form orthonormal bases).

In the classical mathematical definition, the bases are unitary in the sense of the Euclidian norm. It is however well known that for FEM models Euclidian norms do not account for inhomogeneities in the material properties or degree of freedom type (translation/rotation). It is thus more appropriate to consider variants of the singular value decomposition where the bases are orthonormal in the sense of energy norms (Balmes, 1996b). Classically, one will consider left singular vectors that are stiffness orthonormal $U^T K U = I$ and right singular vectors that are orthonormal with respect to the reduced mass $V^T\left[T^M T\right]V = I$. These are simply computed by solving the reduced eigenvalue problem

$$\left[T^T M T\omega_j^2 + T^T K T\right]_{NR\times NR}\{V_j\} = \{0\} \tag{17}$$

and using $s_j = \omega_j^{-2}$ and $U_j = [T]\{V_j\}$.

The largest singular values of this decomposition are associated with the smallest frequencies. On thus obtains the expected result that at equal kinetic energy the most important directions in a subspace are associated with the lowest strain energies and thus lowest frequencies. This demonstrates the intuitive result that in absence of information on loads, the best subspace is associated with modal truncation.

Computing the modes within any reduced subspace T is thus an "optimal" selection method. Since this is a mathematical classification of orthogonal directions in subspace T, the M and K used only need to be representative of the physics of the underlying system.

Finally there is a purely numerical interest in solving (17). While the independence of vectors in basis T is not theoretically needed, the practical use of nearly collinear vectors linked to singular or poorly conditioned matrices. For the considered numerical applications, it is thus essential to guarantee the independence of vectors in T. The singular value decomposition of this matrix leads to orthogonal vectors and nearly collinear vectors can be eliminated by truncating vectors associated with very low singular values.

3 Parametric families of models

3.1 Fixed bases for multiple models

As a first illustration one will consider applications where one seek to build an approximation of the response of not one but multiple models. FEM models are described by a set of geometric and material properties. A parameterized model potentially lets all properties change (node positions, values characterizing the constitutive law, ...). Formally, one can define a vector of parameters in the model

$$\{p\} = \{p_0\} + \{\Delta p\} \tag{18}$$

In practice, one usually defines a coefficient for each element matrix (or sub-matrix when separating membrane and bending matrices for example). The linear combination thus becomes

$$[M(p)] = \sum_{j=1}^{NE} \alpha_k(p)[M_k^e] \quad [K(p)] = \sum_{j=1}^{NE} \beta_k(p)[K_k^e] \tag{19}$$

As will be shown in section 3.2, variations of modal properties are quite non linear. The use of perturbation methods, even of high order, thus does not yield sufficient accuracy. Reanalysis techniques (Tourneau et al., 1994; Balmes, 1996c; Bouazzouni et al., 1997) will thus be preferred here.

These methods seek approximate solutions in a subspace T independent of p by solving for each value of p

$$\left[\left[T^T K(p) T\right] - \omega_{jR}^2(p)\left[T^T M(p) T\right]\right]\{\phi_{jR}(p)\} = \{0\} \tag{20}$$

As long as K and M are a matrix polynomials in p, one can project the matrix coefficients once and for all. The resolution of (20) can thus be very fast. Restitution of responses on all DOFs is then simply given by $\{\phi_j\} = [T]\{\phi_{jR}\}$.

The fundamental question is the procedure to build a basis T giving good predictions for all desired values of p. One can rewrite the problem as the solution of

$$\left[K(p_0) - \omega_j^2 M(p_0)\right]\{\phi_j(p)\} = [Z(p) - Z(p_0)]\{\phi_j(p)\} \tag{21}$$

If the right hand-side in (21) is small enough, the nominal modes $T = [\phi(p_0)_{1:NM}]$ will give an reasonable approximation (Tourneau et al., 1994). This however does not make use of the hypothesis on representative loads.

It can be easily realized that right hand side vectors $[Z(p) - Z(p_0)]\{\phi_j(p)\}$ actually span a low dimension subspace that can be approximated by $b = [\Delta Z]\{\phi_j(p_0)\}$. One can thus combine the basis of nominal modes and first order corrections

$$[T] = \left[\phi(p_0)_{1:NM} \;\; [K(p_0)]^{-1}[[\Delta K]\{\phi_j(p_0)\} \;\; [\Delta M]\{\phi_j(p_0)\}]\right] \tag{22}$$

This basis is very much related (Bobillot and Balmes, 2003; Balmes, 1996c) to the use of a basis containing modes and their sensitivities $T = \left[\phi(p_o) \; \frac{\partial \phi}{\partial p_i}\right]$. As an alternative, the multi-model approach (Balmes, 1996c) retains exact modes at a number of design points p_i, thus $T = [\phi(p_1) \; \phi(p_{NE})]$.

For a basis of nominal modes, predictions are valid for a fairly narrow parametric zone because the reduction basis does not account for actual model variations (Balmes, 1996c). By including sensitivities, one significantly extends the range of validity but this range is not easily controlled. For a multi-model basis, mode shapes predictions are exact for the retained values $p_i, i = 1 : NE$ and fairly good between those points. In the rest of the paper, one considers a basis where one keeps the nominal modes and a number of other design points.

Building a multi-model reduction basis requires exact computations at target design points. The choice of these points is an important problem treated in the design of experiments (Myers and Montgomery, 1995). As shown in figure 3 the

uncertainty intervals are assumed to form an hypercube. A classical experiment would evaluate objectives at all corners, thus leading to 2^{NP} evaluations.

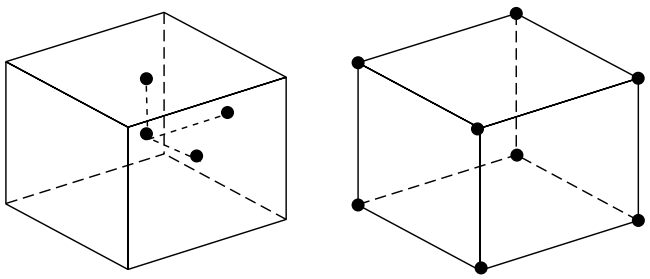

Figure 3: Positions of exact mode evaluations in parameter space. a) Hypercube face center. b) Classical 2^{NP} factorial plan.

Building a multi-model basis using this full experiment is not realistic for the applications of interest. For the ESC-A model shown in figure 4, keeping 15 modes uses 13 MB. Keeping modes for 2^{10} corners of a 10 parameter hypercube would require 13 GB which is not realistic both in terms of disk space and computational time.

The retained experiment uses the exact $NP + 1$ responses at the face centers. This is much more practical but introduces an arbitrary selection of the *upper* face of the hypercube. In practice, one thus verifies the accuracy of reanalysis results on the opposite face using the error evaluation technique outlined in section 3.3.

The basis combining modes computed at each design point is generally poorly conditioned (the vectors are very collinear). One thus uses a complete reorthonormalization of this basis with respect to the nominal mass and stiffness matrices as motivated in section 2.4.

Finally, the uncertainty model to be propagated being defined by the parametric hypercube $p_i \in \left[p_i^{\min} p_i^{\max}\right]$, it is important to validate the precision of reanalysis predictions on the full domain. Possible strategies on the selection of points where this accuracy is estimated will be discussed in section 3.3.

3.2 Application to uncertainty propagation analyses

Quantities of interest for to analyze the controllability of the launcher are modal frequencies and excitabilities. Excitability is defined by the value of j^{th} mode contribution at its resonance frequency, that is

$$e_j = \frac{[c]\{\phi_j\}\{\phi_j\}^T[b]}{2\zeta_j\omega_j^2\omega} \tag{23}$$

For applications, one considered the first 15 modes and 6 excitabilities associated with the transfer between engine gimbal joint and inertial measurements (SRI) in roll (θ_x to θ_x), pitch (u_z to θ_y), and yaw (u_y to θ_z).

One will see later that transmissibilities undergo strong variations during modal crossing. It thus appears important to use concepts derived from MIMO control design methodologies. Rather than considering individual transmissibilities, one can consider the 3 inputs (engine θ_x, u_z, u_y) and 6 outputs (rotations at both SRI). e_j then is a 6×3 matrix whose singular values can be used as objectives since they are much more stable. Similarly for close modes, one can consider the sum of transmissibilities for nearby modes (Balmes, 1997).

The number of computations increasing exponentially with the number of parameters, it is important to only retain parameters that are really necessary. In the initial decomposition into substructures shown in figure 4 a single multiplicative stiffness parameter is retained. This is clearly a rough approximation but finding a logical basis for any aggregation of parameters is difficult. Engineering judgment and analysis of static test results led to retain 10 parameters shown in table 1. Analysis of target mode sensitivities was then used to allow further parameter elimination. The end result of these analyzes is a table giving, for each target modes, the important parameters by order of importance.

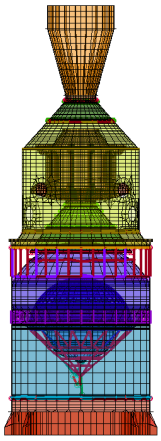

Figure 4: Model decomposition into sub-structures (one color per group).

Table 1: Retained parameters and maximal variations for the first 15 frequencies

#	Name	typ	cur.	min	max	$\max \Delta f$
1	461 ACU Basse	k	1	0.8	1.2	11 % (3)
2	430 Sylda5 court	k	1	0.9	1.1	6 % (12)
3	530 IS Skirt	k	1	0.9	1.1	2 % (15)
4	RLH2 upper	k	1	0.82	1.07	2 % (9)
5	RLH2 lower	k	1	0.82	1.07	1 % (8)
6	410 Case C	k	1	0.9	1.1	1 % (3)
7	481 Cone PPF	k	1	0.95	1.15	0 % (3)
8	520 BMA	k	1	0.95	1.05	1 % (7)
9	ITS	k	1	0.95	2.2	11 % (7)
10	570 Saro	k	1.12	1.12	1.27	1 % (6)

Figure 5a shows evolutions of the first mode frequency. The figure shows the edges of the dimension 4 hypercube associated with parameters 2,3,4,6 as a function of the two parameters inducing the largest variations.

This display is generated using 160 evaluations, which is much below a coverage of the hypercube using random or structured experiments necessary for the constitution of histograms shown in figure 5b, while still giving an excellent indication of the range of variations for the objectives (frequency or excitability).

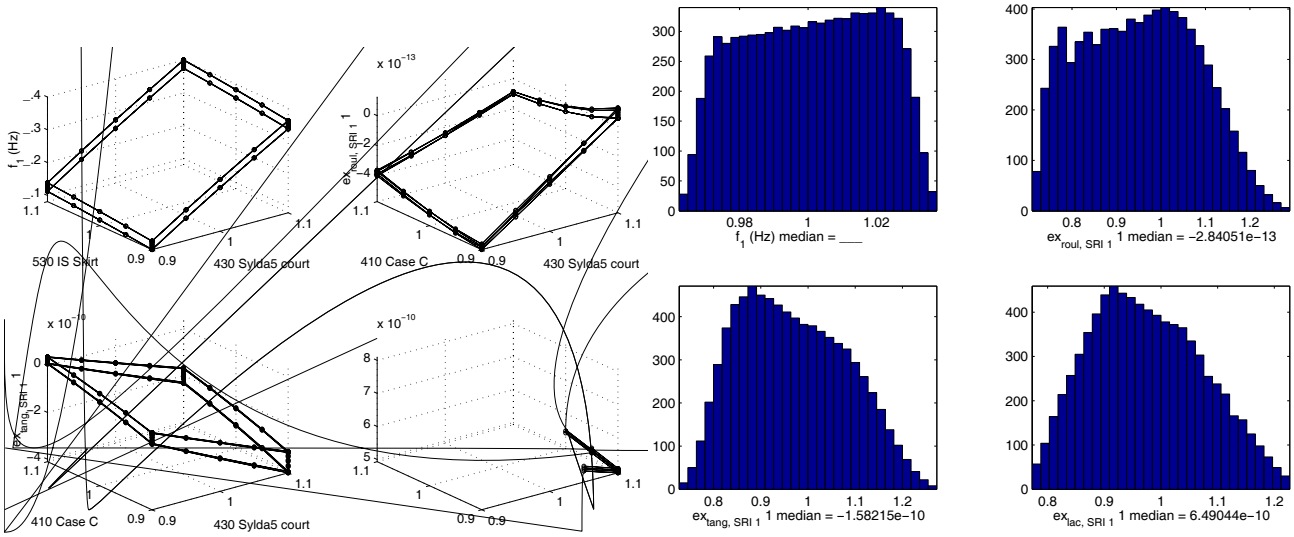

Figure 5: a) Evolution of mode 1 frequency on the edges of a 4 parameter hypercube. b) Corresponding histograms

The first few modes are favorable cases, because they do not lead to modal crossing phenomena. Similar results are obtained for modes that do not show strong sensitivity to parameters. In other cases, one has difficulties illustrated for modes 5-7 in figure 6. There, one clearly sees that the range of variation of ITS properties can lead to two mode crossings. Such behavior could not be reproduced by perturbations or polynomial response surfaces. One will note that reanalysis can be seen as the creation of a response surface characterized by a rational fraction with the inverse of a polynomial dynamic stiffness.

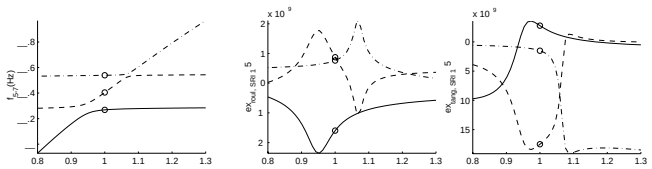

Figure 6: Evolution of frequencies and excitabilities during crossing of modes 5:7 for changes in properties of ITS (Inter Tank Struts). *o* exact values.

3.3 Computational strategies and error control

For the 105 000 DOF model of ESC-A, the evaluation of 15 modes at a parametric point is performed in 80s (PIII 1 GHz Linux, SDT (Balmes and Leclère, 2003) with `spfmex` static solver). A propagation study requiring several thousand points, finding a compromise between accuracy and computational time is an obligation.

For the considered problem, building the reanalysis basis requires 500 s (for 6 full order solution) and reanalysis itself is approximately 1000 faster than a full order solve. The main factor influencing that acceleration is the size of the reanalysis basis, which depends on the number of parameters and the selection of target modes. It is possible to speed computations up by focusing on a small number of target modes that need not be the first few (Balmes, 2004b).

The error evaluation strategy shown in section 2.3 is here only four times faster than an exact result. This is in great part due to the heavy cost of matrix / vector product for the mass matrix that has very large blocks linked to added mass for the fluids. Error evaluation could still be significantly optimized but gaining orders of magnitude is unlikely.

To control error, the initial idea was to select a richer experiment design than for the reanalysis building. A first control is actually performed by checking accuracy levels on negative face centers of the hypercube of figure 3. This check is coupled with the initial sensitivity analysis on parameters.

This first verification does not however validate the effects of correlated variations of multiple parameters. For a small number of parameters, the 2^{NP} factorial experiment (see (Myers and Montgomery, 1995)) associated with the corners of the hypercube gives a good confidence in results. But beyond ten parameters the cost associated with this check becomes prohibitive.

The retained strategy is to check error on points of hypercube edges shown in figure 5a where at least one of the objective scalars reaches an extremum. For this application, extrema of frequency and transmissibility to SRI1 of modes 5-6-7, a number of extrema are reached at the same parametric points which leads to only 16 error evaluations.

Figure 7 shows that errors are small when transmissibilities are important. The few points where transmissibilities are not very small and the error visible could be used to enrich the reanalysis basis. It is interesting to note that the relative error on strain energy is always small ($< 10^{-6}$), which shows that this error is not a good indicator of errors on transmissibilities (local error on shape).

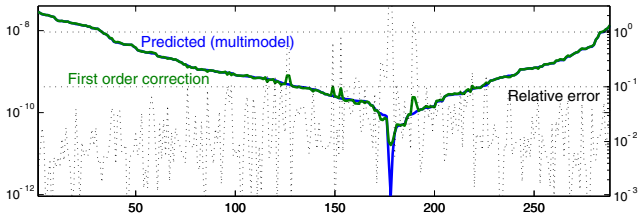

Figure 7: Errors on the prediction of transmissibilities on extreme points of objectives (modes 5:7, 6 parameters). Left scale and continuous lines: predicted values and results with one step enrichment sorted by value. Right scale and dotted line : relative error on the prediction.

4 Modes and coupled systems

4.1 General formulation of coupling

Among the many applications where coupled systems are considered one can cite substructuring, structural dynamic modification, fluid and soil/structure interaction, vibroacoustics, ...

Taking the case of two components to simplify equations with no loss of generality, the two subsystems 1 and 2 can be described by a set of decoupled equations,

$$\begin{bmatrix} Z_1 & 0 \\ 0 & Z_2 \end{bmatrix} \begin{Bmatrix} q_1 \\ q_2 \end{Bmatrix} = \begin{bmatrix} b_1 \\ b_2 \end{bmatrix} \{u(s)\}$$
$$\{y\} = [c_1 \;\; c_2] \begin{Bmatrix} q_1 \\ q_2 \end{Bmatrix} \tag{24}$$

In structure/structure interactions (typically Component Mode Synthesis), the coupling is typically described by an approximation of the continuity condition $X_1(x) = X_2(x)$. For compatible meshes, this is typically enforced through a condition on the equality of DOFs. With incompatible meshes, the general form of continuity conditions derived from strong or weak formulations (Farhat and Géradin, 1992; Ben Dhia and Balmes, 2003) is a set of linear constraints

$$[c_1 \;\; c_2] \begin{Bmatrix} q_1 \\ q_2 \end{Bmatrix} = 0 \tag{25}$$

Enforcing (25) in (24), leads to an overdetermined set of equations. To remain in the framework for Ritz methods, one thus seeks a basis T for the null space of conditions (25) and solves by doing the classical transformation (3) on (24).

There is a widespread misconception on the fact that the left product by T^T corresponds to an application of the action/reaction principle. In Ritz methods, force equilibrium is not verified in a continuous sense. Only the work of assumed displacement that verify continuity conditions, on assumed *virtual* fields that verify the same continuity conditions, is zero. This understanding can be important when considering coupling of incompatible meshes.

A clear interest of defining the coupling condition in the form (25) is that its form remains identical during model reduction. Given approximations of component models $\{q_i\} \approx [T_i]\{q_{R1}\}$, the reduced coupling condition becomes

$$[c_1 T_1 \;\; c_2 T_2] \left\{ \begin{array}{c} q_{R1} \\ q_{R2} \end{array} \right\} = 0 \tag{26}$$

Reduction and component synthesis thus appear as inherently decoupled. It is possible combine free component reduction ((Rubin, 1975) or (MacNeal, 1971) methods with attachment and free interface modes) and fixed component reduction ((Craig and Bampton, 1968) with constraint and fixed interface modes).

Most of the CMS litterature dedicates major efforts to find explicit expressions of the solution of (24) given (25). Using numerical tools to find a basis for the null space of (25) (or (26) for a reduced model) however eliminates the need for such expressions and thus allows for any model reduction. This is in particular useful when dealing with incompatible meshes.

4.2 Illustration on an SDM application

Structural Dynamics Modification is a classical application combining experimental modal analysis and CMS. One performs modal analysis on a base structure and wishes to predict quantitatively the response of a modified structure. Difficulties that are not dealt with by classical SDM theory (Maia and Silva, 1997) are the non coincidence between the modification edge and measurement points and possible errors in the quality of measurements.

The methodology proposed in (Corus, 2003) combines the following ingredients : a local model, mode shape expansion, and subspace selection. Figure 8 gives a typical application to a pump in a nuclear plant. An initial modal test gives a characterization of the response on a number of test nodes. One then designs a modification (here four stiffeners) and seeks to predict their effects.

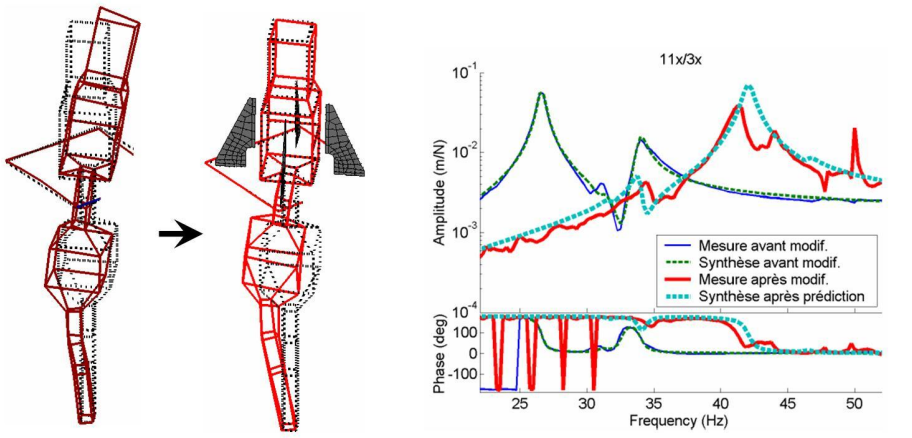

Figure 8: Predictions of the effect of stiffeners on a pump. Modeshape before and after modification. Transfer on the pump head.

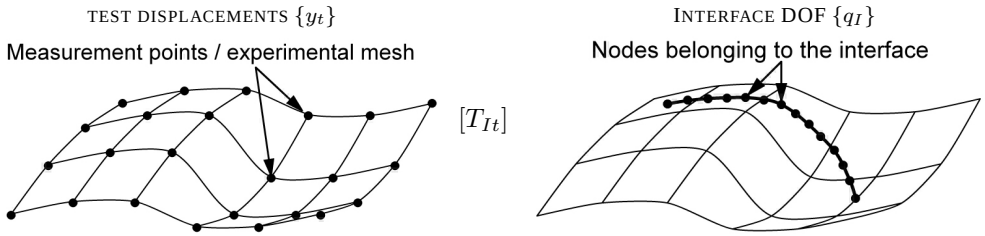

Figure 9: Estimation of $\{q_I\}$ deriving from $\{y_t\}$ using $[T_{It}]$.

To obtain coupled predictions, one must estimate, as shown in figure9, the base structure response at the location of interface degrees of freedom (as shown in the application of figure 8 sensors need not be placed on the interface). One thus seeks to use model reduction to generate a relation of the form

$$\{q_I\} = [T_{It}]\{y_{test}\} \tag{27}$$

This relation which estimates motion at interfaces DOFs given motion at sensors is obtained using two principles presented in section 2. First one defines a local FEM model that matches the geometry of the tested structure but need not be an accurate mechanical representation. One then generates a large subspace of regular shapes of this model by computing static responses to *representative loads* at sensors (associated to observation matrix c_t) and interface DOFs (associated to c_I)

$$[T_G] = [K]^{-1}\left[c_t^T \;\; c_I^T\right]_{N\times(Nt+NI)} \tag{28}$$

since subspace $[T_G]$ contains more shapes than sensors, one then performs a selection of directions $[\phi_G]$ using (17). Criteria to determine the appropriate number of directions to keep in the subspace are discussed in (Corus, 2003).

5 Model reduction for damping predictions

In this final section, one shows how appropriate bases can be introduced to analyze the response of damped structures.

5.1 Handling viscoelastic materials

The basic assumption of linear viscoelasticity is the existence of a relaxation function $h(t)$ such that the stress is obtained as a convolution with the strain history. Using the Laplace transform, one obtains an equivalent representation where the material is now characterized by the *Complex Modulus* E (transform of the relaxation function)

$$\sigma(s) = E(s,T,\epsilon_0)\varepsilon(s) = (E' + iE'')\varepsilon(s) \tag{29}$$

For all practical purposes, one can thus, in the frequency domain, deal with viscoelasticity as a special case of elasticity where the material properties are complex and depend on frequency, temperature, initial deformation and other environmental factors.

Dependence on environmental factors should *a priori* be arbitrary. In practice however, one assumes, and generally verifies, that environmental factors only act as shifts on the frequency (Nashif et al., 1985) (this is the so called *temperature/frequency equivalence principle*). Tests thus seek to characterize a master curve $E_m(s)$ and a shift function $\alpha(T,\epsilon_0)$ describing the modulus as

$$E(s,T,\epsilon_0) = E_m(\alpha(T,\epsilon_0)s) \tag{30}$$

For simulations, a function generating E for all values of s, T, ϵ_0 must be created. As illustrated in figure 10, this function must handle continuations outside of the range of the experimental nomogram, since these are likely to happen in a design study. Useful complements are the ability to generate nomograms (these are standard representations of frequency and temperature dependencies in a single plot (Nashif et al., 1985)), to combine experimental material characterizations into a nomogram, or to estimate the parameters of an analytic representation of a test.

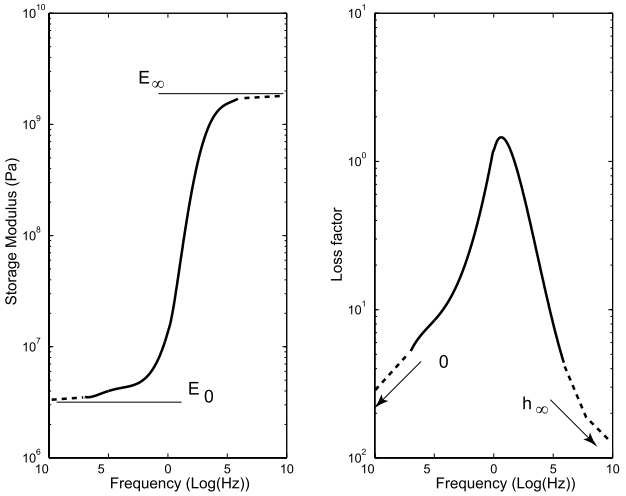

Figure 10: Master curve of a real material

When proper care is taken, both analytical and tabular representations of $E(s)$ are capable of closely approximating material test data. They thus have the same "physical" validity. The differences are really seen in how each representation can be integrated in FEM solvers and in the validity of extrapolations outside the tested material behavior range. On the later point, the actual process used to obtain the parameters has a strong influence, it may thus be easier to obtain a good model with a particular representation even if that representation is not inherently better.

While rational fractions or fractional derivatives (Nashif et al., 1985) are analytical representation of particular interest to implement constant matrix solvers (Golla and Hughes, 1985; McTavish and Hugues, 1987; Lesieutre and Bianchini, 1993; Bianchini and Lesieutre, 1994; Lesieutre and Bianchini, 1995), it was found that all design and validation phases can be handled properly using representations where $E(i\omega)$ is interpolated from tabulated material test data. This is thus the solution retained here.

5.2 Practical solvers for damped vibroacoustic problems

Given a constitutive law described by parameters $E_i(s,T,\epsilon_0)$, one can use the fact that element stiffness matrices depend linearly on those parameters to build a representation of the dynamic stiffness as a linear combination of constant matrices

$$[Z(E_i,s)] = \left[Ms^2 \; + K_e + \textstyle\sum_i E_i(s,T,\epsilon_0) \frac{K_{vi}(E_0)}{E_0} \right] \tag{31}$$

This representation is the basis used to develop practical solvers for viscoelastic vibration problems. Typically, the final predictions of interest are responses at target locations to loads applied on the structure. Assuming that the responses are linearly related to model DOFs by the observation matrix $[c]$, and loads can be decomposed into input shapes $[b]$ and time/frequency dependent inputs $\{u(s)\}$, one must compute

$$\begin{array}{ccc} [Z(E_i,s)]\{q\} & = & [b]\{u(\omega)\} \\ \{y(\omega)\} & = & [c]\{q\} \end{array} \tag{32}$$

at various operating points (values of frequency s, temperature T and/or pre-stress ϵ_0, leading to E_i values).

While most FEM software will handle one instance of problem (32) easily, typical design studies require computation of a few thousand frequency points at tens of design points thus making direct frequency resolution totally impractical. Fixed basis model reduction builds a fixed approximation subspace T and estimates the response using a standard Ritz-Galerkin approximation

$$\{\hat{q}(\omega)\} \approx [T] \left[T^T Z(\omega,T,\epsilon_0) T \right]^{-1} \left[T^T \right] \{F(\omega)\}, \tag{33}$$

Starting with a tangent elastic stiffness $K_0 = Re\left(Z(E_i,0)\right)$, reduction bases that are used classically are

- normal (real) modes of the structure
$$T = [\phi_{1:NM}(K_0)], \tag{34}$$
on can consider modes of a structure with a nominal treatment or modes of the untreated structure and estimate response in the treatment by static condensation.

- normal (real) modes of the structure with a first order static correction for the viscoelastic loads generated by these shapes (Plouin and Balmes, 2000)
$$T = \left[\phi_{1:NM}(K_0) \;\; K_0^{-1} \mathrm{Im}(Z(\omega_0, E_{i0}))\phi_j \right], \tag{35}$$

- higher order bases resulting from the Residual Iteration process described in section 2.3.

Each of these approximations is used successively in the design process. Nominal modes for placement, the first order correction (35) for parametric optimization and higher order iterative solutions for the final validations.

Figure 11 shows a typical averaged transfer function with tracking of resonances. Such computations typically require the resolution of (32) at thousands of frequency points and tens of design points. Using fixed reduced bases to build the parametric model is thus critical for proper operation.

The range of validity of such parametric models is of course a sensitive issue. Figure 12 shows a pole tracking performed for a temperature robustness study. The frequency/damping curves show a typical bell shaped behaviour but also seem to diverge at lower temperatures. Lower temperatures correspond to higher stiffness and one can demonstrate (Merlette et al., 2004) that this divergence can be systematic if the reduction basis is built with a value of the modulus that is too low.

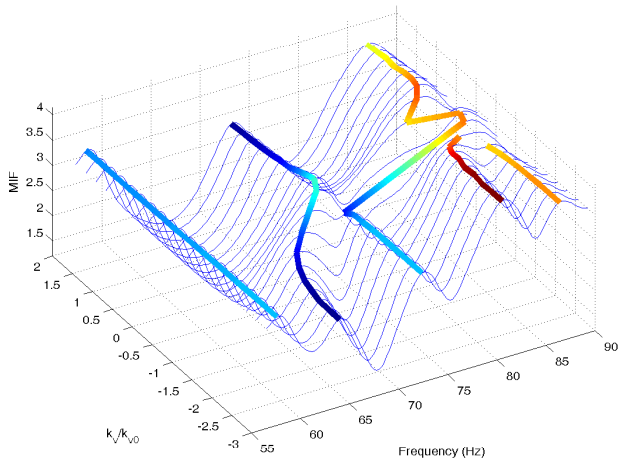

Figure 11: Mode indicator function found when optimizing layer properties (Balmes, 2004a).

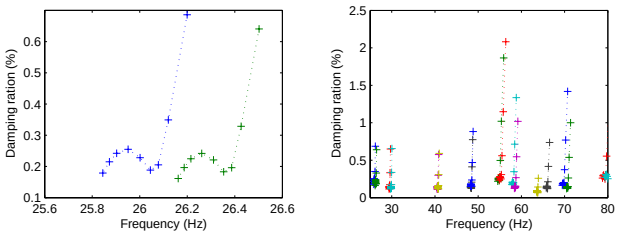

Figure 12: Pole tracking on the -40+40^oC range (Floor panel, case B1/SM50e (Balmes and Germès, 2002))

5.3 Extensions for vibroacoustic predictions

In many practical cases, the final prediction of interest is a vibroacoustic response where the structure is coupled with a compressible non-weighing fluid, with or without a free surface. Using a finite element formulation for this type of problem, leads (Morand and Ohayon, 1992) to equations of the form

$$\left[\begin{bmatrix} M & 0 \\ C^T & K_p \end{bmatrix} s^2 + \begin{bmatrix} K(s) & -C \\ 0 & F \end{bmatrix}\right] \begin{Bmatrix} q \\ p \end{Bmatrix} = \begin{Bmatrix} F^{ex} \\ 0 \end{Bmatrix} \tag{36}$$

with q the displacements of the structure, p the pressure variations in the fluid and F^{ex} the external load applied to the structure.

Given a reduction basis T_s for the structure, one builds a reduction basis containing fluid modes within the bandwidth of interest and static corrections for the effects of vectors in T_s. Thus the resulting basis for the fluid model is

$$[T_f] = \left[\phi_{f,1:NM} \;\; [F]^{-1}[C]^T[T_s]\right] \tag{37}$$

Similar equations can of course be developed for applications where the fluid is represented using boundary elements (Kergourlay et al., 2000).

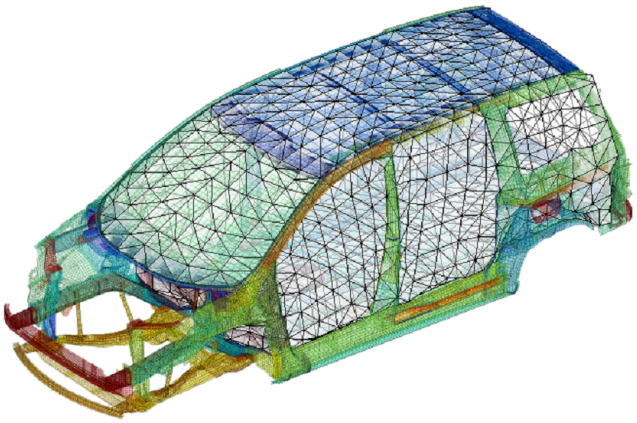

Figure 13: Solid model of the C8 body and fluid model of the interior cavity. (Balmes and Germès, 2004).

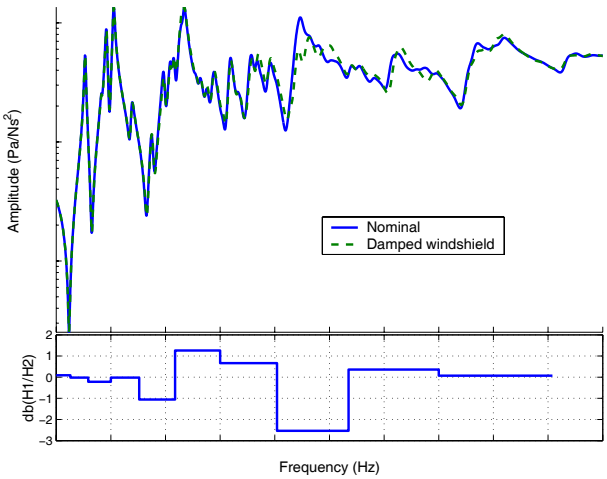

Figure 14: Effect of windshield damping on the vibroacoustic response of automotive body.

In automotive applications, validations will often include vibroacoustic predictions. Figure 13 shows the models of a Citroen C8 body. The solid model uses approximately 1e6 DOFs, 200 000 Nodes and elements, 100 000 linear constraints.

The fluid model contains 2400 nodes and 10 000 elements. Since the solid model is not closed, openings in the body are assumed infinitely rigid.

The target transfers are from load applied on two engine mounts to four locations representative of passenger ear locations. 304 for structural modes up to 225 Hz are retained for frequency response predictions. Figure 14 shows a typical study of interest, where one compares acoustic levels for configurations without and with windshield damping.

6 Conclusion

The need to include modeshapes and static responses to representative loads has been shown to be fundamental in building accurate model reduction techniques. Error estimation and subspace classification then give very general mechanisms to develop new procedures as illustrated on a range of examples.

References

Balmes, E. (1996a). De l'utilisation de la norme en énergie pour la création de modèles réduits en dynamique des structures. *C. R. Acad. Sci. , Paris, 323, Série IIb*, pages 255–260.

Balmes, E. (1996b). Optimal ritz vectors for component mode synthesis using the singular value decomposition. *AIAA Journal*, 34(6):1256–1260.

Balmes, E. (1996c). Parametric families of reduced finite element models. theory and applications. *Mechanical Systems and Signal Processing*, 10(4):381–394.

Balmes, E. (1997). *Modèles analytiques réduits et modèles expérimentaux complets en dynamique des structures*. Mémoire d'habilitation à diriger des recherches soutenue à l'Université Pierre et Marie Curie.

Balmes, E. (2000). Review and evaluation of shape expansion methods. *International Modal Analysis Conference*, pages 555–561.

Balmes, E. (2004a). Incorporating damping predictions in the vibroacoustic design process. *ISMA, Leuven*.

Balmes, E. (2004b). Uncertainty propagation in experimental modal analysis. *IMAC, Dearborn*.

Balmes, E. and Germès, S. (2002). Tools for viscoelastic damping treatment design. application to an automotive floor panel. *ISMA*.

Balmes, E. and Germès, S. (2004). Design strategies for viscoelastic damping treatment applied to automotive components. *IMAC, Dearborn*.

Balmes, E. and Leclère, J. (2003). *Structural Dynamics Toolbox 5.1 (for use with MATLAB)*. SDTools, Paris, France, www.sdtools.com.

Barthe, D., Deraemaeker, A., Ladevèze, P., and Loch, S. L. (2004). Validation and updating of models of industrial structures based on the constitutive relation error. *AIAA Journal*, 42(7):1427–1434.

Ben Dhia, H. and Balmes, E. (2003). Mesure de compatibilité et application aux problèmes de sous-structuration. *Colloque National en Calcul des Structures, Giens*.

Bianchini, E. and Lesieutre, G. (1994). Viscoelastic constrained-layer damping - time domain finite element modeling and experimental results. *SDM Conference, AIAA paper 94-1652-CP*, pages 2666–2676.

Bobillot, A. (2002). *Méthodes de réduction pour le recalage. Application au cas d'Ariane 5*. PhD thesis, Ecole Centrale de Paris.

Bobillot, A. and Balmes, E. (2002a). Expansion par minimisation du résidu dynamique. résolution et utilisation pour la localisation d'erreur. *Revue Européenne des Éléments Finis*.

Bobillot, A. and Balmes, E. (2002b). Iterative techniques for eigenvalue solutions of damped structures coupled with fluids. *SDM Conference*.

Bobillot, A. and Balmes, E. (2003). Iterative computation of modal sensitivities. *Accepted by AIAA Journal*.

Bouazzouni, A., Lallement, G., and Cogan, S. (1997). Selecting a ritz basis for the reanalysis of the frequency response functions of modified structures. *Journal of Sound and Vibration*, 199(2):309–322.

Chouaki, A., Ladevèze, P., and Proslier, L. (1998). Updating Structural Dynamic Models with Emphasis on the Damping Properties. *AIAA Journal*, 36(6):1094–1099.

Corus, M. (2003). *Amélioration des méthodes de modification structurale par utilisation de techniques d'expansion et de réduction de modèle*. PhD thesis, École Centrale Paris.

Craig, R. J. (1987). A review of time-domain and frequency domain component mode synthesis methods. *Int. J. Anal. and Exp. Modal Analysis*, 2(2):59–72.

Craig, R. J. and Bampton, M. (1968). Coupling of substructures for dynamic analyses. *AIAA Journal*, 6(7):1313–1319.

Farhat, C. and Géradin, M. (1992). A hybrid formulation of a component mode synthesis method. *33rd SDM Conference, AIAA Paper 92-2383-CP*, pages 1783–1796.

Farhat, C. and Géradin, M. (1998). On the general solution by a direct method of a large-scale singular system of linear equations: Application to the analysis of floating structures. *International Journal for Numerical Methods in Engineering*, 41:675–696.

Golla, D. and Hughes, P. (1985). Dynamics of viscoelastic structures – a time domain finite element formulation. *Journal of Applied Mechanics*, 52:897–906.

Guyan, R. (1965). Reduction of mass and stiffness matrices. *AIAA Journal*, 3:380.

Kergourlay, G., Balmes, E., and Clouteau, D. (2000). Interface model reduction for efficient fem/bem coupling. *International Seminar on Modal Analysis, Leuven*.

Lesieutre, G. and Bianchini, E. (1993). Time domain modeling of linear viscoelasticity using augmenting thermodynamic fields. *SDM Conference, AIAA paper 93-1550-CP*, pages 2101–2109.

Lesieutre, G. and Bianchini, E. (1995). Time domain modeling of linear viscoelasticity using augmenting thermodynamic fields. *J. Vibration and Acoustics*, 117:424–430.

MacNeal, R. (1971). A hybrid method of component mode synthesis. *Computers and structures*, 1(4):581–601.

Maia, N. and Silva, J. (1997). *Theoretical and Experimental Modal Analysis*. John Wiley & Sons.

McTavish, D. and Hugues, P. (1987). Finite element modeling of linear viscoelastic structures. *ASME Biennal Conference on Mechanical Vibration and Noise*.

Merlette, N., Germes, S., van Herpe, F., Jezequel, L., and Aubry, D. (2004). The use of suitable modal bases for dynamic prediction of structures containing high damping materials. *ISMA, Leuven*, pages 619–633.

Morand, H. J.-P. and Ohayon, R. (1992). *Fluid Structure Interaction*. J. Wiley & Sons 1995, Masson.

Myers, R. H. and Montgomery, D. C. (1995). *Response Surface Methodology*. Wiley Inter Science, New York.

Nashif, A., Jones, D., and Henderson, J. (1985). *Vibration Damping*. John Wiley and Sons.

Plouin, A. and Balmes, E. (2000). Steel/viscoelastic/steel sandwich shells. computational methods and experimental validations. *International Modal Analysis Conference*, pages 384–390.

Rubin, S. (1975). Improved component-mode representation for structural dynamic analysis. *AIAA Journal*, 13(8):995–1006.

Tourneau, P., P., B., Mercier, F., and Klein, M. (1994). Applications of scatter analyses in satellite development. *CNES/ESA International Conference* Spacecraft structures and mechanical testing, *Cepadues Editions*.

Verdun, P. and Balmes, E. (2003). Prospadd : outil d'aide à l'atténuation de la réponse vibro-acoustique des structures. *AAAF Convergence*.

Responsibility notice

The author is the only responsible for the printed material included in this paper.